

# Thermal Buckling of a Fire-Damaged Composite Column Exposed to Heat Flux

Liu Liu\* and George A. Kardomateas†

Georgia Institute of Technology, Atlanta, Georgia 30332-0150

DOI: 10.2514/1.18164

This paper deals with the thermal buckling of a fire-damaged composite column, which is exposed to heat flux from one side. The column is composed of an undamaged layer and a fire-damaged layer (char layer), which is due to the resin material decomposition during fire. Two end fixity cases are considered: an axially restrained column (constrained, immovable ends case) and a column free to move axially (unconstrained case). The column is exposed to heat flux from the fire-damaged layer side, and this results in a nonuniform transient temperature distribution. To simplify the thermal conduction problem, we treat it as one-dimensional in the direction of thickness. For the thermal buckling analysis, the mechanical properties of the fire-damaged region (char) are considered negligible; the degradation of the elastic properties with temperature in the undamaged layer (especially near the glass transition temperature of the matrix) is accounted for, by using experimental data for the elastic modulus of the glass/vinyl-ester material as a function of temperature. Furthermore, the formulation includes transverse shear. Because of the nonuniform stiffness, the effect of the ensuing thermal strains and the resulting eccentric loading, the structure behaves like an imperfect column and responds by bending rather than buckling in the classical bifurcation (Euler) sense. Simple equations for the response of the column are derived and numerical results are presented for the deflection with the variation of time. Two possible transverse deformation modes are identified, one is the column bending toward the heat source, and the other is the column bending away from the heat source. Which direction the column bends is determined by the competition between the thermal moment and the eccentricity moment. Finally, the effect of the fire-damaged (char) layer is assessed by comparison with the original (without fire-damage) column.

## Nomenclature

$a$	=	thickness of the char
$E$	=	extensional modulus
$G$	=	shear modulus
$H$	=	thickness of the column
$h_i$	=	relative heat transfer coefficient
$i$	=	1 for the undamaged layer; 2 for the char
$K_i$	=	thermal conductivity
$L$	=	length of the column
$l$	=	thickness of the undamaged layer
$M_z^T$	=	thermal moment resultant
$M_z^e$	=	eccentricity moment
$N_x^T$	=	thermal force resultant
$Q$	=	impending heat flux
$T_0$	=	temperature of the surrounding air, also initial temperature
$v_i$	=	temperature
$w$	=	transverse deflection
$x$	=	lengthwise coordinate
$y$	=	thicknesswise coordinate
$\beta$	=	shear correction factor
$\kappa_i$	=	thermal diffusivity

## I. Introduction

OF considerable concern is the resulting effect of catastrophic events such as fire or explosions on the integrity of structures. In addition to the implications for design, quantitative information regarding the nature of the strength loss is required to make decisions

regarding, for example, the seaworthiness of a ship that has sustained fire damage. In particular, it is of current interest to know such a response in structures made out of advanced fiber reinforced composites, because these materials are used at an ever increasing pace in aerospace, marine, infrastructure and chemical processing applications.

In fact, much data on the fire properties of composites exist, including ignition times, heat release rates, smoke production rates, and gas emissions (Sorathia et al [1,2]; Egglestone and Turley [3]; Scudamor [4]; Gibson and Hume [5]; Brown and Mathys [6]; Mouritz and Gardiner [7]). On the contrary, there is little research done on the structural behavior and integrity during and following exposure to fire. One of the few studies on this subject is by Mouritz and Gardiner [7], who studied the effect of fire damage on the edgewise compression properties and failure mechanisms of sandwich composites and found large reductions to the edgewise compression properties of phenolic-based sandwich composites despite having good flame resistance. Still, the combined effect of simultaneous mechanical loading and thermal (fire) loading has not been studied. This paper addresses this issue as far as compressive loading, which in an otherwise purely mechanical loading (no fire) would lead to bifurcational (Euler) buckling. In addition, this paper includes the effect of char (decomposed layer) which has a significant influence on the temperature distribution and also on the resulting structural response.

As far as the undamaged layer, the temperature distribution still induces a considerable spatial change in stiffness, therefore the layer is essentially a nonhomogeneous material. This is because an important characteristic of fiber reinforced polymeric composites is that increases in temperature cause a gradual softening of the polymer matrix material with a profoundly significant effect near the glass transition temperature  $T_g$ . In this study we use the data from recent experiments on E-glass vinyl-ester composites, conducted by Kulkarni and Gibson [8], as a basis for including the effect of the resulting nonuniform stiffness distribution.

Therefore, when fire is applied on one side of a column/plate, two things happen: first, a char (damaged) layer appears and, second, a nonuniform temperature develops through the thickness of the undamaged layer. These two effects result in a nonuniform

Received 12 June 2005; revision received 20 March 2006; accepted for publication 31 March 2006. Copyright © 2006 by the American Institute of Aeronautics and Astronautics, Inc. All rights reserved. Copies of this paper may be made for personal or internal use, on condition that the copier pay the \$10.00 per-copy fee to the Copyright Clearance Center, Inc., 222 Rosewood Drive, Danvers, MA 01923; include the code \$10.00 in correspondence with the CCC.

\*Graduate Research Assistant.

†Professor of Aerospace Engineering. Associate Fellow AIAA

distribution of stiffness through the thickness. In addition, a thermal moment is developed, which causes bending of the column from the very start of fire when only the slightest change of temperature occurs. Thus, the column bends like a beam (even if it is initially straight) and cannot buckle in the classical Euler (bifurcation) sense. In this paper, we investigate the general bending response of such a column that is pinned at both ends, with an applied axial force. We consider two cases: immovable ends, which would result in axial reaction forces due to the thermal loading and ends free to move axially under the action of an applied axial load. The details of the formulation are outlined next.

## II. Formulation

### A. Temperature Distribution

We now consider a composite column consisting of an undamaged layer and a char layer, as shown in Fig. 1. Coordinates axes  $x$  and  $y$  are chosen as shown in Fig. 1. We assume that the column is exposed to a constant heat flux from the right surface and the left surface has a "radiation" boundary condition to the surrounding media. To simplify the analysis, the temperature of the surrounding air at the left surface is denoted by  $T_0$ , the column is assumed to be initially at  $T_0$  and the thermal boundary conditions at  $x = 0$  and  $x = L$  are assumed to be adiabatic, so that the heat conduction problem becomes a one-dimensional one governed by the  $y$  coordinate.

Let us denote by  $K_1$ ,  $\kappa_1$ ,  $h_1$  and  $v_1$  the conductivity, diffusivity, relative heat transfer coefficient, and temperature for the undamaged composite column in the region  $-l \leq y \leq 0$  and by  $K_2$ ,  $\kappa_2$  and  $v_2$  the corresponding quantities for the char layer in the region  $0 \leq y \leq a$ .

The differential equations for the temperature field are

$$\frac{\partial^2 v_1}{\partial y^2} - \frac{1}{\kappa_1} \frac{\partial v_1}{\partial t} = 0 \quad \text{at } -l \leq y \leq 0, \quad t > 0 \quad (1a)$$

$$\frac{\partial^2 v_2}{\partial y^2} - \frac{1}{\kappa_2} \frac{\partial v_2}{\partial t} = 0 \quad \text{at } 0 \leq y \leq a, \quad t > 0 \quad (1b)$$

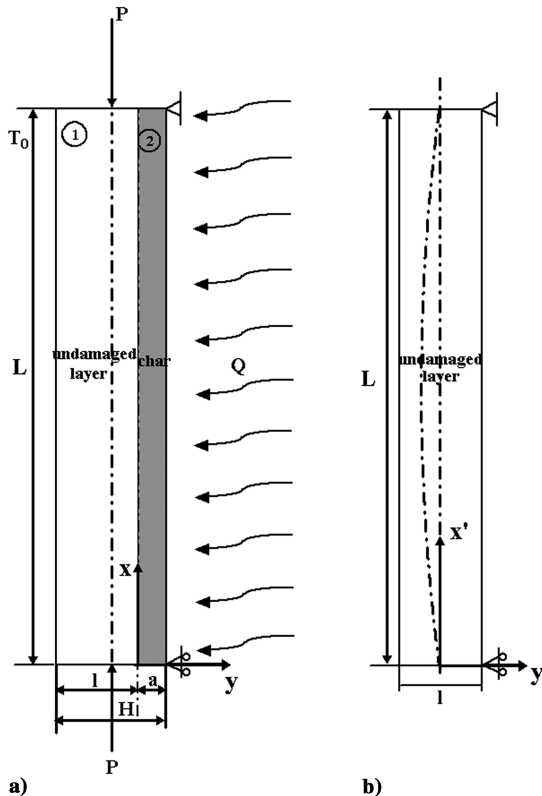


Fig. 1 Definition of the geometry for a fire-damaged (charred) column under heat flux  $Q$ .

If we assume there is no contact resistance at the surface of separation between the char and the undamaged layer  $x = 0$ , then the thermal conditions at that surface are

$$K_1 \frac{\partial v_1}{\partial y} = K_2 \frac{\partial v_2}{\partial y} \quad \text{at } y = 0, \quad t > 0 \quad (2a)$$

$$v_1 = v_2 \quad \text{at } y = 0, \quad t > 0 \quad (2b)$$

For the composite column described above, the initial condition can be written as

$$v_1 = v_2 = T_0 \quad \text{at } -l \leq y \leq a, \quad t = 0 \quad (2c)$$

the boundary conditions of  $Q$  at the fire side  $y = a$ :

$$-K_2 \frac{\partial v_2}{\partial y} = -Q \quad \text{at } y = a, \quad t > 0 \quad (2d)$$

and the boundary condition of radiation to a medium at temperature  $T_0$  at the other side  $y = -l$ :

$$\frac{\partial v_1}{\partial y} = h_1(v_1 - T_0) \quad \text{at } y = -l, \quad t > 0 \quad (2e)$$

If we set:

$$\tilde{v}_1 = \Delta T_1 = v_1 - T_0$$

$$\tilde{v}_2 = \Delta T_2 = v_2 - T_0$$

then  $\tilde{v}_1$  and  $\tilde{v}_2$  satisfy Eq. (1), (2a), (2b), and (2d); but the initial condition (2c) and the boundary condition (2e) should be rewritten as

$$\tilde{v}_1 = \tilde{v}_2 = 0 \quad \text{at } -l \leq y \leq a, \quad t = 0 \quad (3a)$$

and

$$\frac{\partial \tilde{v}_1}{\partial x} = h_1 \tilde{v}_1 \quad \text{at } y = -l, \quad t > 0 \quad (3b)$$

With the aid of the Laplace transformation for the time  $t$  we now analyze the temperature change governed by Eqs. (1a) and (1b). Denoting the Laplace transform of  $F(t)$  as  $\bar{F}(p)$  and taking into account the initial condition (3a), the equation for the temperature change in the transformed domain can be written as

$$\frac{d^2 \bar{v}_1}{dy^2} - q_1^2 \bar{v}_1 = 0 \quad \text{at } -l \leq y < 0 \quad (4a)$$

$$\frac{d^2 \bar{v}_2}{dy^2} - q_2^2 \bar{v}_2 = 0 \quad \text{at } 0 < y \leq a \quad (4b)$$

where  $q_1 = (p/\kappa_1)^{1/2}$ ,  $q_2 = (p/\kappa_2)^{1/2}$ .

These have to solved with the following corresponding boundary conditions:

$$K_1 \frac{d\bar{v}_1}{dy} = K_2 \frac{d\bar{v}_2}{dy} \quad \text{at } y = 0 \quad (5a)$$

$$\bar{v}_1 = \bar{v}_2 \quad \text{at } y = 0 \quad (5b)$$

$$\frac{d\bar{v}_2}{dy} = \frac{Q}{K_2 p} \quad \text{at } y = a \quad (5c)$$

$$\frac{d\bar{v}_1}{dy} = h_1 \bar{v}_1 \quad \text{at } y = -l \quad (5d)$$

The solution of Eq. (4) is

$$\bar{v}_1(y, q_1) = A_1 \cosh(q_1 y) + B_1 \sinh(q_1 y) \tag{6a}$$

$$\bar{v}_2(y, q_2) = A_2 \cosh(q_2 y) + B_2 \sinh(q_2 y) \tag{6b}$$

We use the notation  $\kappa = \sqrt{\kappa_1/\kappa_2}$ ,  $K = K_2/K_1$ , then  $q_2$  can be replaced by  $\kappa q_1$ .  $A_1, B_1, A_2$ , and  $B_2$  are unknown constants, which can be determined from the boundary conditions, Eqs. (5). Substituting Eq. (6) into Eqs. (5) results in the following equations for the determination of these unknown constants:

$$B_1 q_1 - K B_2 q_1 \kappa = 0 \tag{7a}$$

$$A_1 - A_2 = 0 \tag{7b}$$

$$A_2 \kappa q_1 \sinh(\kappa q_1 a) + B_2 \kappa q_1 \cosh(\kappa q_1 a) = \frac{Q}{K_2 p} \tag{7c}$$

$$\begin{aligned} &[-q_1 \sinh(q_1 l) - h_1 \cosh(q_1 l)]A_1 + [q_1 \cosh(q_1 l) \\ &+ h_1 \sinh(q_1 l)]B_1 = 0 \end{aligned} \tag{7d}$$

These equations can be represented in matrix form:

$$\begin{bmatrix} 0 & 0 & a_{13} & a_{14} \\ a_{12} & a_{22} & 0 & 0 \\ a_{31} & 0 & a_{33} & 0 \\ 0 & a_{42} & 0 & a_{44} \end{bmatrix} \begin{bmatrix} A_1 \\ B_1 \\ A_2 \\ B_2 \end{bmatrix} = \frac{Q}{K_2 p} \begin{bmatrix} 1 \\ 0 \\ 0 \\ 0 \end{bmatrix} \tag{8}$$

where the nonzero elements  $a_{ki}$  of the coefficient matrix  $[a_{ki}]$  are given as follows:

$$a_{13} = \kappa q_1 \sinh(\kappa q_1 a); \quad a_{14} = \kappa q_1 \cosh(\kappa q_1 a) \tag{9a}$$

$$\begin{aligned} a_{21} &= -q_1 \sinh(q_1 l) - h_1 \cosh q_1 l \\ a_{22} &= q_1 \cosh(q_1 l) + h_1 \sinh q_1 l \end{aligned} \tag{9b}$$

$$a_{31} = 1; \quad a_{33} = -1 \tag{9c}$$

$$a_{42} = q_1; \quad a_{44} = -K \kappa q_1 \tag{9d}$$

Then the temperature solution in the transformed domain can be written as

$$\bar{v}_1(y, p) = \frac{Q}{K_2 p} \frac{A_1 \cosh(q_1 y) + B_1 \sinh(q_1 y)}{\Delta} \tag{10a}$$

$$\bar{v}_2(y, p) = \frac{Q}{K_2 p} \frac{A_2 \cosh(q_2 y) + B_2 \sinh(q_2 y)}{\Delta} \tag{10b}$$

where  $\Delta = |a_{ki}| = \det(a_{ki})$ .

From the inversion theorem, the solution for the temperature distribution is found to be

$$\tilde{v}_1(y, \lambda) = \frac{Q}{K_2} \int_{\gamma-i\infty}^{\gamma+i\infty} \frac{A_1 \cosh(q_1 y) + B_1 \sinh(q_1 y)}{\lambda \Delta} e^{\lambda t} d\lambda \tag{11a}$$

$$\tilde{v}_2(y, \lambda) = \frac{Q}{K_2} \int_{\gamma-i\infty}^{\gamma+i\infty} \frac{A_2 \cosh(q_2 y) + B_2 \sinh(q_2 y)}{\lambda \Delta} e^{\lambda t} d\lambda \tag{11b}$$

where  $\lambda$  is written in place of  $p$  in Eq. (10) to emphasize the fact that in Eq. (11) we are considering the behavior of  $\tilde{v}_1$  and  $\tilde{v}_2$  regarded as functions of a complex variable.

Using the residue theorem, we can accomplish the inverse Laplace transformation of Eq. (11); then the temperature solutions  $\tilde{v}_1$  and  $\tilde{v}_2$  are given by the summation of the residues. Because the residue for

$\lambda = 0$  gives a solution for steady state, we treat separately the single-value poles of Eq. (11) corresponding to  $\lambda = 0$  and the roots of  $\Delta = 0$ .

Let us denote

$$\lambda_n = -\kappa_1 \alpha_n^2; \quad q_1 = i \alpha_n; \quad \lambda_n = \kappa_1 q_1^2, \quad n = 1, 2, 3 \dots \tag{12}$$

where  $\pm \alpha_n, n = 1, 2, 3 \dots$  are the roots (all real and simple) of

$$\Delta = 0 \tag{13}$$

Then the transient part of temperature solution  $\tilde{v}_1$  and  $\tilde{v}_2$  is given as

$$\tilde{v}_1 = \frac{Q}{K_2} \sum_{n=1}^{+\infty} \frac{2e^{\kappa_1 q_1^2 t}}{q_1 \Delta'} [A_1 \cosh(q_1 y) + B_1 \sinh(q_1 y)]_{q_1=i\alpha_n} \tag{14a}$$

$$\tilde{v}_2 = \frac{Q}{K_2} \sum_{n=1}^{+\infty} \frac{2e^{\kappa_1 q_1^2 t}}{q_1 \Delta'} [A_2 \cosh(q_1 y) + B_2 \sinh(q_1 y)]_{q_1=i\alpha_n} \tag{14b}$$

where  $\Delta'$  is the derivative of the determinant  $\Delta(\lambda)$  with respect to  $\lambda$ . Finally  $\tilde{v}_1$  and  $\tilde{v}_2$  can be written as functions of  $t$  and  $y$  in terms of  $\alpha_n$ .

Next, we determine the steady temperature solution  $\tilde{v}_1$  and  $\tilde{v}_2$ . From Eq. (1), the governing equations for  $\tilde{v}_1$  and  $\tilde{v}_2$  are

$$\frac{\partial^2 \tilde{v}_1}{\partial y^2} = 0 \quad \text{at } -l \leq y < 0, \quad t > 0 \tag{15a}$$

$$\frac{\partial^2 \tilde{v}_2}{\partial y^2} = 0 \quad \text{at } 0 < y \leq a, \quad t > 0 \tag{15b}$$

Then the resulting solution for  $\tilde{v}_1$  and  $\tilde{v}_2$  can be written in the following form:

$$\tilde{v}_1 = \bar{A}_1 y + \bar{B}_1 \tag{16a}$$

$$\tilde{v}_2 = \bar{A}_2 y + \bar{B}_2 \tag{16b}$$

where  $\bar{A}$  and  $\bar{B}$  are the unknowns constants determined so as to satisfy boundary conditions.

Combining the steady and transient parts, we have the complete temperature solution  $\tilde{v}_1$  and  $\tilde{v}_2$ , as

$$\begin{aligned} \tilde{v}_1 &= \Delta T_1 = \left( \frac{Q}{K_1} y + \frac{1 + h_1 l}{h_1} \frac{Q}{K_1} \right) \\ &+ \frac{Q}{K_2} \sum_{n=1}^{\infty} \frac{2e^{\kappa_1 q_1^2 t} [A_1 \cosh(q_1 y) + B_1 \sinh(q_1 y)]}{q_1 \Delta'} \Big|_{q_1=i\alpha_n} \end{aligned} \tag{17a}$$

$$\begin{aligned} \tilde{v}_2 &= \Delta T_2 = \left( \frac{Q}{K_2} y + \frac{1 + h_1 l}{h_1} \frac{Q}{K_1} \right) \\ &+ \frac{Q}{K_2} \sum_{n=1}^{\infty} \frac{2e^{\kappa_1 q_1^2 t} [A_2 \cosh(q_1 y) + B_2 \sinh(q_1 y)]}{q_1 \Delta'} \Big|_{q_1=i\alpha_n} \end{aligned} \tag{17b}$$

The first part of the equation represents the steady state solution and the second part of the equation represents the transient solution. In theory, the numerical solution of the above problem can always be obtained because of the series factor  $\exp(-\kappa_1 \alpha_n^2 t)$ , which is uniformly convergent when  $t \geq t_0 > 0$ ;  $t_0$  being any positive number. In practice, the solution requires a reasonable number of terms for convergence for moderate and large values of  $t$ .

### B. Thermal Buckling

We now consider the thermal buckling problem of the column, which has been exposed to fire. In this part, the analysis is based on the same assumptions as these made by Mouritz and Gardiner [7], which assume the mechanical properties of the char region are

negligible because of the thermal decomposition of polymer matrix; the mechanical properties of the undamaged region are the same as the mechanical properties of the original (unburned) composite with the effect of temperature included. Therefore, the thermal buckling analysis is based only on the undamaged composite column and the temperature field in the undamaged region, as derived in the previous section, which, nevertheless, is influenced by the presence of the char layer, is used in the following.

Regarding the stiffness  $E$  of the composite column, it is well known that the modulus of polymers depends strongly on the temperature and especially on how close the temperature is to the glass transition temperature  $T_g$ . For composites with polymeric matrices, it is logical to expect the stiffness  $E$  depends on temperature. In a recent paper, Kulkarni and Gibson [8] studied the effects of temperature on the elastic modulus of E-glass/vinyl-ester composites, and provided measurements of temperature dependence of the elastic modulus of the composite in the range of 20 to 140°C. The glass transition temperature of the matrix was  $T_g = 130^\circ\text{C}$ . Near this temperature the Young's modulus shows a significant variation but well below  $T_g$  the variation is small. If we denote by  $E_0$  the modulus at room temperature  $T_0 = 20^\circ\text{C}$  then the data in Kulkarni and Gibson [8] fit the following equation, where  $E(T)$  is the modulus at the temperature  $T$  (Fig. 2):

$$\begin{aligned} \frac{E}{E_0} &= 1 - a_1 \left( \frac{T - T_0}{T_g - T_0} \right) + a_2 \left( \frac{T - T_0}{T_g - T_0} \right)^2 - a_3 \left( \frac{T - T_0}{T_g - T_0} \right)^3 \\ &= 1 - a_1 \left( \frac{\Delta T_1}{\Delta T_g} \right) + a_2 \left( \frac{\Delta T_1}{\Delta T_g} \right)^2 - a_3 \left( \frac{\Delta T_1}{\Delta T_g} \right)^3 \end{aligned} \quad (18)$$

For the present E-glass/vinyl-ester,  $E_0 = 3 \times 10^8 \psi = 20.6$  GPa and  $a_1 = 0.348$ ,  $a_2 = 0.715$ , and  $a_3 = 0.843$ . The composite studied has a fiber volume fraction of 0.516 and a  $[(0/45/90/-45/0)]_2$  ply layup. The above equation captures the physics of the nonlinear dependence of the composite on the glass transition temperature of the matrix  $T_g$ . To simplify the formulations in the thermal buckling analysis, the axis  $x$  is transmitted to the midsurface of the undamaged layer  $y = -\ell/2$ , as shown in Fig. 1.

In the new coordinate system, we define an ‘‘average’’ modulus  $E_{av}$  and ‘‘a first and second moment’’ of the modulus with respect to the midsurface  $y$  axis,  $E_{m1}$  and  $E_{m2}$  respectively by

$$E_{av}A = \int_A E \, dA; \quad E_{m1}\ell A = \int_A E y \, dA; \quad E_{m2}I = \int_A E y^2 \, dA \quad (19)$$

where  $A$  is the cross sectional area,  $a$  is the thickness of the undamaged layer, and  $I$  is the moment of inertia ( $I = \int_A y^2 \, dA$ ). The integral is evaluated numerically as a simple closed form expression cannot be obtained.

Because of the nonuniform modulus, the neutral axis of the column is not at the midsurface. The distance  $e$  of the neutral axis from the midsurface axis  $x$  is determined from

$$e \int_A E(y) \, dA = \int_A E(y)y \, dA \quad (20)$$

which, by use of Eq. (19) leads to

$$e = E_{m1}\ell/E_{av} \quad (21)$$

Assuming the thermal expansion coefficient  $\alpha$  independent of temperature, the thermal force is

$$N_x^T = \int_A E\alpha\Delta T_1 \, dA \quad (22a)$$

which, by use of Eqs. (17a) and (18), can be evaluated numerically.

The thermal force can be developed due to the constraints at both ends of the beam, which causes the column to buckle; however, the problem is not a bifurcation because a thermal moment is also developed. The thermal moment (with respect to the neutral axis of

the beam) is

$$M_z^T = \int_A E\alpha\Delta T_1(y - e) \, dA \quad (22b)$$

and this would cause bending of the column.

Besides that, eccentric loading can cause another bending moment, the value of which is

$$M_z^e = P e' = P \left( e + \frac{a}{2} \right) \quad (22c)$$

where the eccentric distance  $e' = e + a/2$  is different from the distance  $e$  derived from Eq. (21), because the applied force or the constraint force is applied at the centroid of the entire column including the fire-damaged and undamaged layers, whereas the coordinate axis  $x$  was defined at the midsurface of the undamaged layer  $y = -\ell/2$ . This eccentricity moment would cause bending either in the same or the opposite sense of the thermal moment.

The problem now is to determine the response of the column under the influence of  $N_x^T$ ,  $M_z^T$ , and  $M_z^e$ , which changes the character of the problem from bifurcation buckling to a bending problem. That is, if the applied axial load is large enough to constrain the column at both ends, the column will bend as the  $M_z^T$  and  $M_z^e$  are applied. Of course, the applied force  $P$  could cause failure if it is large enough. Specifically, as the load increases, the column midspan  $w$  increases until the column fails due to the bending.

We consider two cases: one is the column is constrained by the two ends, which cannot move (constrained or immovable ends case); the other is that the column is free to displace axially and is acted upon by a constant applied compressive load  $P$ . First of all, let us assume that both ends are immovable and let us denote by  $P$  the external support (or reaction) force. The axial force  $N_x$  does not vary with the axial position  $x$  (Simitis [9]). Thus, it can be seen that  $N_x^T$  equal to  $-P$ , due to axial equilibrium. However, unlike the case of a uniformly heated column, the force  $P$  is less than  $N_x^T$  because of the thermal moment  $M_z^T$  and the eccentricity moment  $M_z^e$ . That is, the column bends away from its original straight configuration due to  $M_z^T$  and  $M_z^e$ , which relieves some of the external support force at the immovable ends. In this case,  $P$  is a derived quantity, not a controlled quantity. The controlled quantity is the thermal loading due to the fire, and the response quantity is the midspan transverse deflection of the column.

Let us denote by  $u_0$  and  $w_0$  the displacements along the  $x$  and  $y$  directions at the neutral axis and by  $\theta$  the rotation of the cross section due to bending. The nonlinear strain at the neutral axis,  $y = e$ , is

$$\epsilon_0(x) = u_{0,x} + \frac{1}{2}\theta^2 \quad (23a)$$

In the following, we account for transverse shear following the procedure in Huang and Kardomateas [10]. In particular, we can set

$$\frac{dw}{dx} = \sin(\theta + \gamma_{eq}) \quad (23b)$$

where  $\gamma_{eq}$  is the equivalent shear angle, that is, the difference between the slope of the deflected beam axis and the rotation  $\theta$  of the cross section due to bending.

It is reasonable to assume  $G$  will change with temperature in the same manner as  $E$ , that is, we can write

$$\begin{aligned} G(y) &= G_0 \left[ 1 - a_1 \left( \frac{T - T_0}{T_g - T_0} \right) + a_2 \left( \frac{T - T_0}{T_g - T_0} \right)^2 - a_3 \left( \frac{T - T_0}{T_g - T_0} \right)^3 \right] \\ &= G_0 \left[ 1 - a_1 \left( \frac{\Delta T_1}{\Delta T_g} \right) + a_2 \left( \frac{\Delta T_1}{\Delta T_g} \right)^2 - a_3 \left( \frac{\Delta T_1}{\Delta T_g} \right)^3 \right] \end{aligned} \quad (23c)$$

An effective shear modulus,  $\bar{G}$  is now defined based on the shear compliance as [10]:

$$\frac{a}{\bar{G}} = \int_{-a/2}^{a/2} \frac{dy}{G(y)} \quad (23d)$$

The equivalent shear angle  $\gamma_{\text{eq}}$  is then defined as

$$\gamma_{\text{eq}} = \frac{\beta P \sin \theta}{\bar{G}A} \quad (23e)$$

where  $\beta$  accounts for the nonuniform distribution of shear stresses throughout the cross section.

Then, the strain at an arbitrary point  $\bar{\epsilon}(x, y)$  can be represented by

$$\bar{\epsilon}(x, y) = \epsilon_0(x) - (y - e) \frac{d(\theta + \gamma_{\text{eq}})}{dx} \quad (23f)$$

When the resulting force from Eq. (23f) is integrated through the section, the resultant should equal  $-P + N_x^T$ , that is

$$\int_A E(y) \bar{\epsilon}(x, y) dA = -P + N_x^T \quad (23g)$$

Then, (23g) becomes by use of Eqs. (23a) and (23e)

$$E_{\text{av}} A (u_{0,x} + \frac{1}{2} \theta^2) + (E_{\text{av}} e - E_{m1} h) A \left( 1 + \frac{\beta P \cos \theta}{\bar{G}A} \right) \theta_{,x} = N_x^T - P \quad (23h)$$

By use of Eq. (21) this results in

$$u_{0,x} = \frac{N_x^T - P}{E_{\text{av}} A} - \frac{1}{2} \theta^2 \quad (23i)$$

which we can integrate over the length of the column subject to the boundary conditions that the ends are restrained in the axial direction, that is  $u_0(0) = 0$  and  $u_0(L) = 0$ . Therefore, we obtain the following:

$$(N_x^T - P) \frac{L}{E_{\text{av}} A} - \frac{1}{2} \int_0^L \theta^2 dx = 0 \quad (23j)$$

which is applicable for the entire loading range of the column and is a ‘‘constraint equation,’’ expressing the condition that the overall change in displacement between the end supports must be zero because the two ends of the beam are immovable.

Now, the bending rigidity  $(EI)_{\text{eq}}$  of the column is likewise influenced by the nonuniform stiffness due to temperature distribution and is defined by

$$(EI)_{\text{eq}} = \int_A E(y) (y - e)^2 dA \quad (24a)$$

By use of Eq. (19), this results in

$$(EI)_{\text{eq}} = E_{m2} I - \frac{E_{m1}^2 h^2 A}{E_{\text{av}}} \quad (24b)$$

Next, we shall modify the beam equation to consider the thermal loading and moderately large deflections. Transverse shear will also be included. In doing so, we shall properly modify the equations developed in Huang and Kardomateas [10]. The moment equation with the thermal effect included, is given by

$$M = -(EI)_{\text{eq}} \frac{d\theta}{dx} - M_z^T \quad (24c)$$

From equilibrium, taking into account the (compressive) applied force  $P$  at both ends, the moment at any position is given by

$$M = Pw + M_0 + M_z^e \quad (24d)$$

where  $M_0$  is the moment at  $x = 0$  and the last term represents the additional moment due to the load being applied eccentrically, Eq. (22c).

Differentiating Eqs. (24c) and (24d) with respect to  $x$  and using Eqs. (23b) and (23e) with the additional assumption that the shear angle is small, so that  $\sin \gamma_{\text{eq}} \simeq \gamma_{\text{eq}}$  and  $\cos \gamma_{\text{eq}} \simeq 1$ , results in

$$(EI)_{\text{eq}} \frac{d^2 \theta}{dx^2} + P \left( \frac{\beta P}{2AG} \sin 2\theta + \sin \theta \right) + \frac{dM_z^T}{dx} = 0 \quad (24e)$$

As far as the ends (simple supports), we have the moment boundary conditions of:

$$\begin{aligned} -(EI)_{\text{eq}} \frac{d\theta}{dx}(0) - M_z^T &= M_z^e = P \left( e + \frac{a}{2} \right) \\ -(EI)_{\text{eq}} \frac{d\theta}{dx}(L) - M_z^T &= M_z^e = P \left( e + \frac{a}{2} \right) \end{aligned} \quad (24f)$$

### C. Linear Analysis

In the following, we shall linearize the differential equation Eq. (24e) and derive a closed form and relatively simple solution. This is actually a reasonable approach, if we consider the fact that the thermal expansion coefficient  $\alpha$  is small enough, which means the  $M_z^T$  influence on the rotation  $\theta$  is correspondingly small. Taking into account the fact that  $M_z^T$  is independent of  $x$ , and linearizing,  $\sin \theta \simeq \theta$ , results in the differential equation

$$(EI)_{\text{eq}} \frac{d^2 \theta}{dx^2} + P \left( \frac{\beta P}{AG} + 1 \right) \theta = 0 \quad (25a)$$

together with the boundary conditions Eq. (24f).

If we set

$$\lambda^2 = \frac{P}{(EI)_{\text{eq}}} + \frac{\beta P^2}{(EI)_{\text{eq}} AG} \quad (25b)$$

then the solution is as follows:

$$\theta(x) = \frac{M_z^T + M_z^e}{\lambda (EI)_{\text{eq}}} \left[ \frac{(1 - \cos \lambda L)}{\sin \lambda L} \cos \lambda x - \sin \lambda x \right] \quad (25c)$$

Notice that the symmetry condition  $\theta(L/2) = 0$  is satisfied automatically in Eq. (25c).

The constraint equation (23j), again linearizing,  $\cos \theta \simeq 1$  becomes

$$(N_x^T - P) \frac{L}{E_{\text{av}} A} - \frac{(M_z^T + M_z^e)^2 (1 - \cos \lambda L)}{2[(EI)_{\text{eq}} \lambda]^2 \sin \lambda L} \left( \frac{L}{\sin \lambda L} - \frac{1}{\lambda} \right) = 0 \quad (25d)$$

The vertical deflection of the beam is obtained for the linear problem by using Eqs. (23b) and (23e) and integrating:

$$w(x) = \left( 1 + \frac{\beta P}{\bar{G}A} \right) \int_0^x \theta(\xi) d\xi \quad (25e)$$

Substituting Eq. (25c) gives

$$w(x) = \frac{M_z^T + M_z^e}{(EI)_{\text{eq}} \lambda^2} \left( 1 + \frac{\beta P}{\bar{G}A} \right) \left[ \frac{(1 - \cos \lambda L)}{\sin \lambda L} \sin \lambda x + (\cos \lambda x - 1) \right] \quad (25f)$$

Notice that from Eq. (25f), the deflections at the ends are zero (as they should),  $w(0) = w(L) = 0$ , and that the midpoint deflection  $w(L/2) = v_m$  is

$$v_m = \frac{M_z^T + M_z^e}{(EI)_{\text{eq}} \lambda^2} \left( 1 + \frac{\beta P}{\bar{G}A} \right) \left[ \frac{1}{\cos(\lambda L/2)} - 1 \right] \quad (25g)$$

and tends to infinity for  $\lambda L = \pi$  (the Euler load of the column).

If the thermal loading is prescribed via the fire heat influx  $Q$ , then  $N_x^T$  and  $M_z^T$  can be determined and the only unknown in Eq. (25f) is  $P$  [or  $\lambda$  from Eq. (25b)]. Then we can solve the transcendental Eq. (25d) for  $P$  and thus obtain the relationship between the thermal loading  $Q$  and  $w$ . This relationship is obtained for constrained columns only and in this case  $P$ , which is obtained from Eq. (25d), is the support

**Table 1** Material properties

Property	Undamaged	Char
$\kappa_i$ , m <sup>2</sup> /s	$1.73 \times 10^{-7}$	$6.85 \times 10^{-8}$
$K_i$ , W/m · K	0.316	0.123
$h_i$ , W/m <sup>2</sup>	10.0	—
$\alpha_i$ , 1/°C	$18.0 \times 10^{-6}$	—
$E_i$ , Pa	$20.6 \times 10^9$	—
$G_i$ , Pa	$2.1 \times 10^9$	—

reaction. On the other hand, if the “constraint” condition of immovable supports is released (second case of ends free to move axially), then  $P$  is the applied load and the relationship between the midpoint deflection  $w_m$  and the applied load  $P$  can be obtained from Eq. (25g). Note also that for zero  $M_z^T$ , the constraint Eq. (25d) reduces to  $N_x^T = P$ , that is, the solution for a uniformly heated column.

### III. Results and Discussion

To illustrate the previous analysis, numerical results are presented for a column that has been exposed to fire and includes both a fire-damaged (char) and an undamaged layer, and the original column without a char layer, to show the influence of the fire-damaged (char) layer on the temperature distribution and the mechanical response. Let us consider these two columns with the same dimensions. The charred one is essentially a column made of two different materials, the undamaged (original) layer and the fire-damaged layer (char), respectively, which have different material properties as shown in Table 1. For the fire-damaged layer (char), the thermal properties are taken from experimental measurements,<sup>‡</sup> the mechanical properties are given by room temperature which is  $T_0 = 20^\circ\text{C}$ ; The other column is the original column without a fire-damaged (char) layer and the original material is E-glass/vinyl-ester. The fire-damaged material (char) has a  $K_i$  much lower than that of the undamaged layer,<sup>§</sup> therefore it is the char that acts as an insulating front. The two columns are shown in Figs. 1 and 3. Let us assume the column dimensions: length  $L = 0.15$  m, thickness,  $H = 0.0125$  m, and width  $b = 0.025$  m. For the charred column, we assume the thickness of fire-damaged (char) layer  $a = H/4$ .

In Fig. 4, we show the temperature distribution of the column with a char layer at different times  $t$ ; the column is subjected to a constant external heat flux  $Q = 10$  kW/m<sup>2</sup>. The temperature distribution in the undamaged layer is emphasized by the darker lines. It is obvious that the temperature increases with the time  $t$ . Although part of resin material decomposes and this creates a char (fire-damaged) layer, the temperature in the undamaged layer is much lower than that in the damaged layer.

To present the influence of the fire-damaged (char) layer and, in particular, the difference of the temperature distributions for the charred and the original columns, we show the temperature distributions for both columns in Figs. 5 and 6. It is obvious that under the same heat flux  $Q = 5$  kW/m<sup>2</sup>, the temperature in the undamaged layer of the charred column is much lower than the temperature in the original column without the fire-damage (char) layer. The reason for such a difference is due to the protection of the fire-damaged layer on the remaining material. The char acts as an insulating front. Furthermore, the net temperature variation in the charred column is smaller than that in the original one, and this has a subsequent direct influence on the resulting thermal moment and the transverse deflection of the column.

In Fig. 7, we show the axial constraint force  $P_{\text{con}}$  for the charred column, which is pinned at both ends (immovable) and subjected to an heat flux  $Q = 10$  kW/m<sup>2</sup> as a function of time  $t$  from 20–300 s. The force  $P_{\text{con}}$  is normalized with the Euler critical load  $P_{\text{Euler}}$  of the column at room temperature. We make a quasistatic assumption, so that the temperature distribution in the undamaged layer can be determined at each fixed time from Eq. (17a). We can see that the

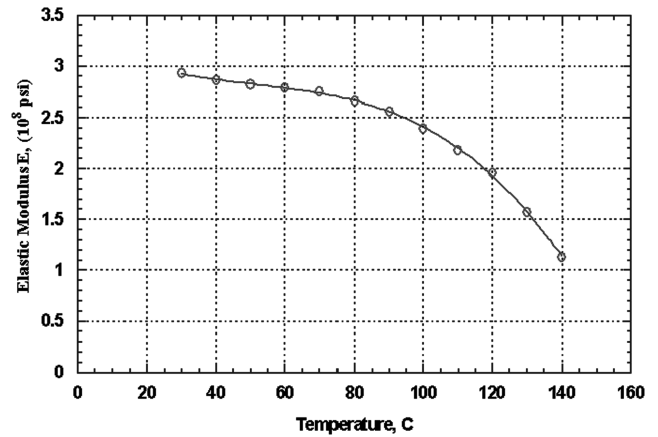


**Fig. 2** The effects of temperature on the elastic modulus of E-glass/vinyl-ester composites.

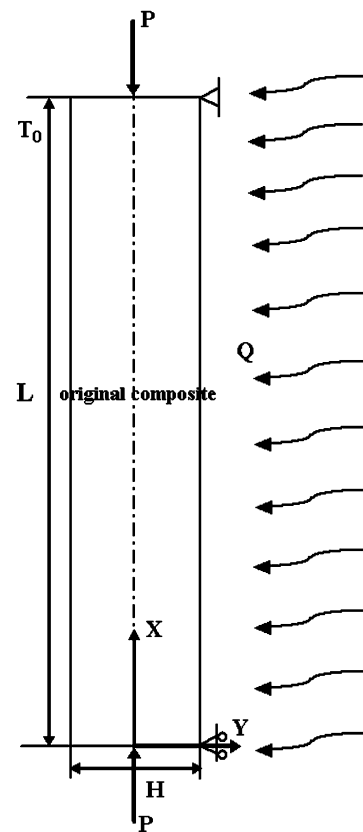


**Fig. 3** Definition of the geometry for the original column, which is exposed to a heat flux  $Q$ .

axial constraint force increases with time  $t$  as  $t < 240$  s; but as  $t > 240$  s,  $P_{\text{con}}$  decreases with exposure time. The variation of the axial constraint force  $P_{\text{con}}$  with time is nonlinear, which is due to the material properties decreasing with the exposure time nonlinearly, as well as due to the fact that the ends are restrained, therefore, beyond a certain level of deformation, the structure starts to “pull” from the ends rather than “push” against the ends.

Based on the axial support force  $P_{\text{con}}$  obtained, the midpoint deflection  $w_m$  is calculated from Eq. (25g). In Fig. 8 we show the midpoint transverse deformation  $w_m$ , which is normalized by  $L$ . We can see that  $w_m$  varies with exposure time nonlinearly. At the beginning of the time exposure, the positive midpoint transverse displacement increases with time. From the definition of the geometry of the structure, the positive transverse displacement means that the column bends toward the heat flux. After the positive  $w_m$  reaches a peak value, it decreases with exposure time and the

<sup>‡</sup>Lattimer, B. Y., private communication, 2005.

<sup>§</sup>Lattimer, B. Y., private communication, 2005.

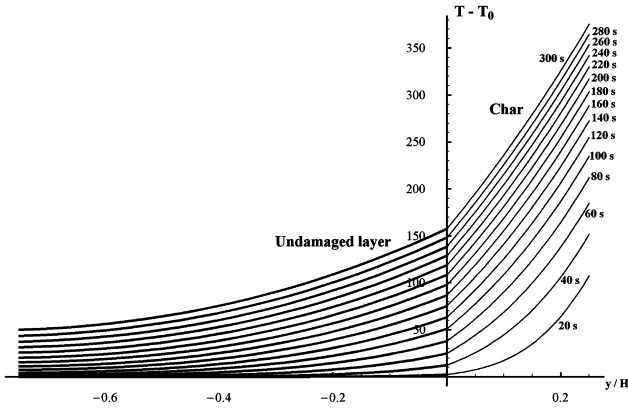


Fig. 4 Temperature distribution of the charred column subjected to heat flux  $Q = 10 \text{ kW/m}^2$ .

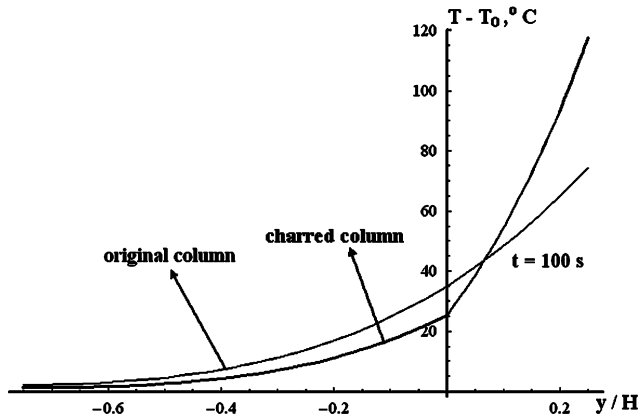


Fig. 5 Temperature distributions for the charred and the original columns subjected to heat flux  $Q = 5 \text{ kW/m}^2$  at  $t = 100 \text{ s}$ .

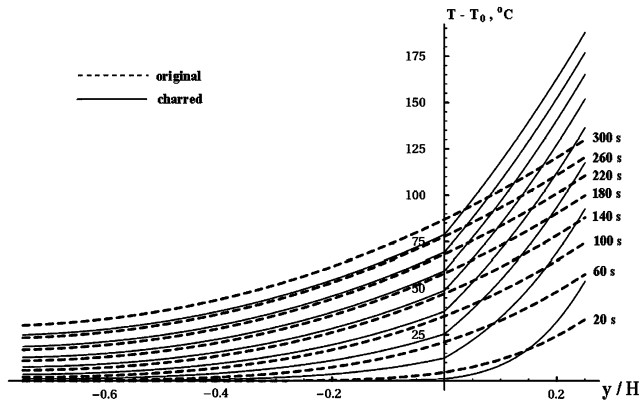


Fig. 6 Temperature distributions for the charred and the original columns subjected to heat flux  $Q = 5 \text{ kW/m}^2$ .

direction of the deformation switched from positive to negative, which shows that if the exposure time is long enough, the column would bend away from the heat flux.

To explain the variation of  $w_m$ , we have to show the variations of the thermal moment and the moment due to the eccentric loading, because the transverse deformation is determined by the overall bending moment  $M_z^e$ . These are shown in Figs. 9 and 10, respectively. It can be seen that the thermal moment is always positive and increases initially with exposure time  $t$ , but it reaches a peak value, and then it begins to decrease; however, its direction does not switch. The thermal moment is determined by the temperature distribution  $\Delta T_1$  and the material stiffness constant  $E$ . At the beginning of the heat exposure,  $E$  did not change very much as

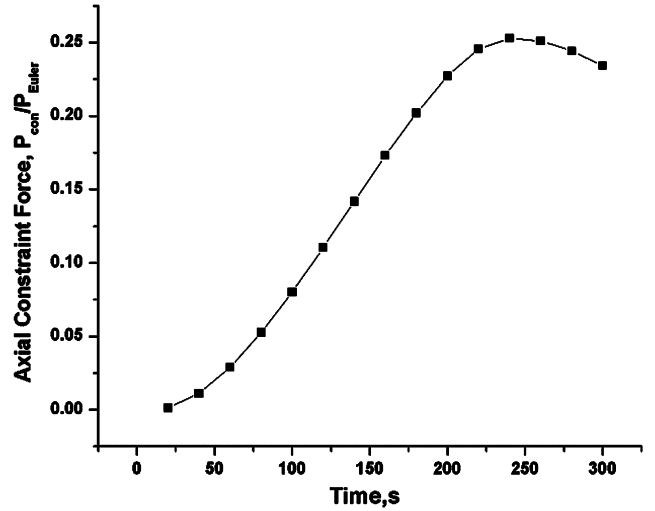


Fig. 7 Axial constraint force  $P_{con}$  vs time for the charred column subjected to heat flux  $Q = 10 \text{ kW/m}^2$ .

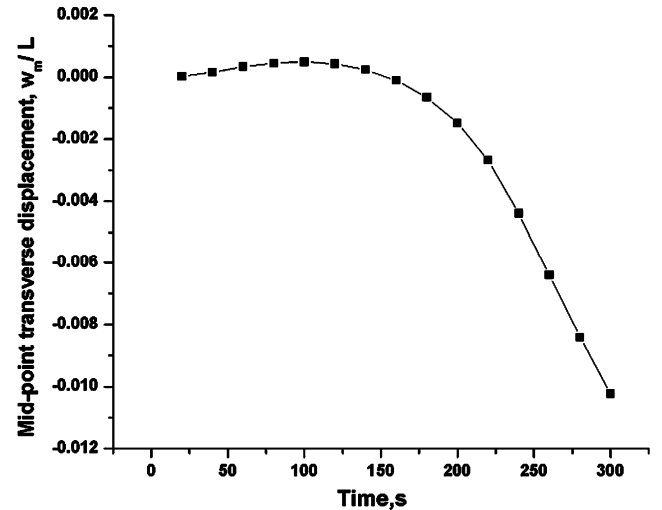


Fig. 8 Midpoint transverse deflection  $w_m$  vs time for the charred column subjected to heat flux  $Q = 10 \text{ kW/m}^2$  (constrained, immovable ends case).

shown in Fig. 2, and the temperature variation dominated the thermal moment, so that the thermal moment increased with exposure time. As the exposure time increased further,  $E$  decreased significantly as the temperature reached the glass transition temperature  $T_g$ ; in this case  $M_z^T$ , is dominated by both  $\Delta T_1$  and  $E$  variations and decreased after a peak value, but its direction did not switch and was always positive. The transverse deformation  $w$  was dominated by the overall moment including  $M_z^T$  and  $M_z^e$  as shown in Eq. (22c). The moment  $M_z^e$  is associated with the eccentric distance  $e$  and the axial force  $P_{con}$  at each time. As shown in Fig. 7, the axial force  $P_{con}$  for the constraint column was positive and always increased, and, as shown in Fig. 10, the eccentric distance  $e$  was negative and the absolute value always increased with the exposure time. And so the direction of the moment  $M_z^e$  was opposite to  $M_z^T$  and the absolute value always increased. The transverse deformation  $w$  was determined by the overall moment  $M_z$ . At the beginning,  $w_m$  is positive and increased because it was dominated by the thermal moment, but later  $w_m$  began to decrease and the direction switched from positive to negative, which means  $w_m$  was governed by  $M_z^e$ .

This foregoing discussion shows that there exist two possibilities, one is the constraint column bends toward the heat source at the beginning of heat exposure due to the dominance of  $M_z^T$ ; the other possibility is the column bends away from the heat source with increasing heat exposure time, as the eccentricity moment begins to

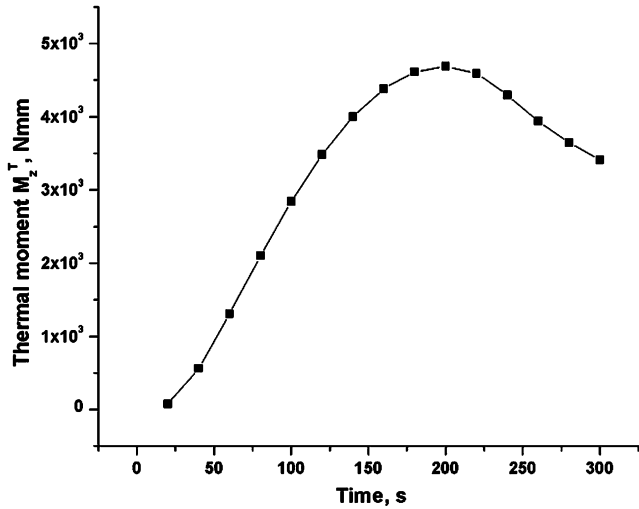


Fig. 9 The thermal moment  $M_z^T$  vs exposure time for the charred column subjected to heat flux  $Q = 10 \text{ kW/m}^2$  (constrained, immovable ends case).

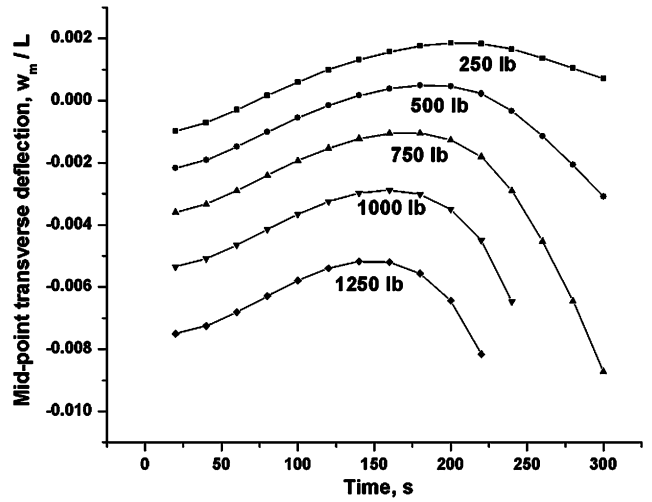


Fig. 11 Midpoint transverse deflection  $w_m$  vs exposure time  $t$  under a constant applied axial force  $P$  (ends free to move axially, unconstrained case). Each curve represents the column response under a constant heat flux  $Q = 10 \text{ kW/m}^2$  and axial force  $P$ .

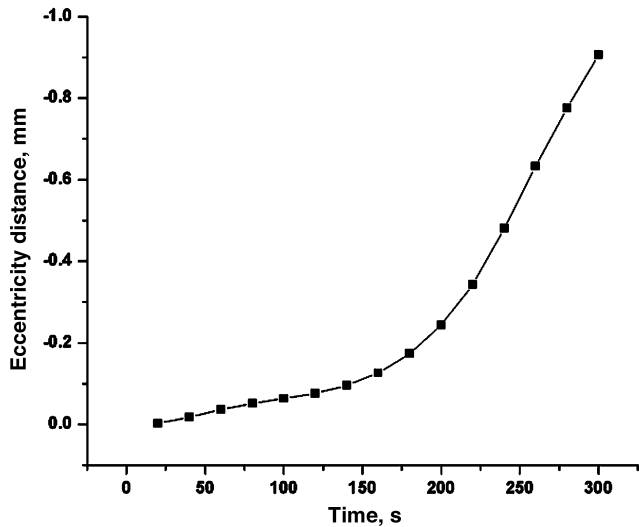


Fig. 10 The eccentricity distance  $e$  vs exposure time for the charred column subjected to heat flux  $Q = 10 \text{ kW/m}^2$  (constrained, immovable ends case).

dominate. Furthermore, all results in Fig. 8 show the consistency between the linear assumption we made to obtain the results and the results themselves, because the midpoint deformation is very small compared with the length of the column, which means that the cross sectional rotation angle  $\theta$  is also quite small. And so we can conclude that the deformation under the temperature distribution is very small and a linear assumption can be made.

In Fig. 11, each curve presents a plot of  $w_m$  vs  $t$ , under a constant applied axial force  $P$ . Here,  $w_m$  is normalized by  $L$ . Each curve represents the column response under a constant heat flux,  $Q = 10 \text{ kW/m}^2$  and axial force  $P$ . The end of the column can move axially freely (unconstrained case). Because of that, the constraint boundary conditions are released, and the constraint condition Eq. (25d) is not applicable; instead,  $P$  is a given variable now. This case differs from the constraint case because for the constraint column, the axial constraint force  $P_{con}$  increased with  $t$  as shown in Fig. 8, but in Fig. 11, for each curve,  $P$  is kept constant from the beginning to the end of exposure. The midpoint transverse deflection  $w_m$ , under the constant heat flux  $Q$  and axial force  $P$ , can be determined from Eq. (25g). The midpoint transverse displacement  $w_m$ , was negative at the beginning of heat exposure, because the moment  $M_z^e$  dominated, but as  $t$  increased, the negative  $w_m$  decreased due to the thermal moment  $M_z^T$ , which increased and influenced  $w_m$ .

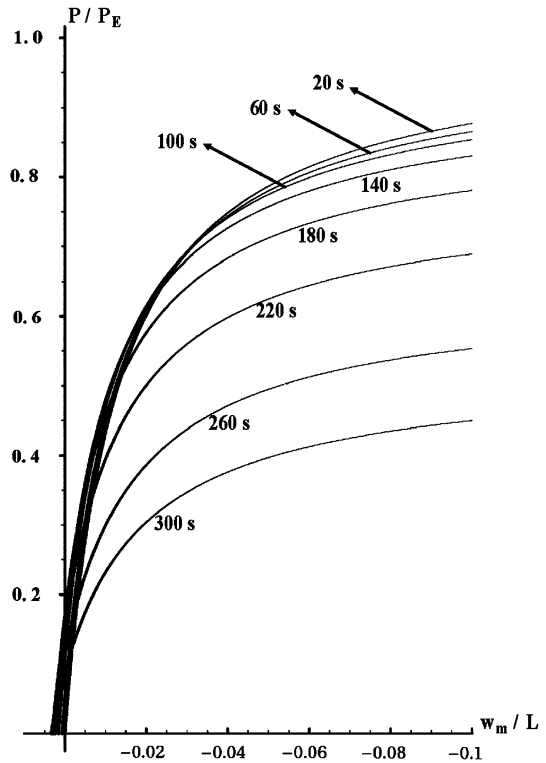


Fig. 12 Applied axial force vs midpoint transverse deflection for the charred column subjected to heat flux  $Q = 10 \text{ kW/m}^2$  at different times  $t$  (ends free to move axially, that is, unconstrained case).

For some curves for example  $P = 250 \text{ lb}$  and  $P = 500 \text{ lb}$ ,  $w_m$  switched in direction from negative to positive, because  $M_z^T$  eventually dominated; for the rest of the curves,  $w_m$  did not change direction because  $M_z^e$  always dominated due to the larger applied axial force. With  $t$  increasing further,  $M_z^e$  began to dominate  $w_m$ , which lead to the positive  $w_m$  decreasing and the negative  $w_m$  increasing. All of these variations were determined from the competition of  $M_z^T$  and  $M_z^e$ . It should be noted that if  $P$  is large enough and the heat exposure time is long enough, then the midpoint transverse deflection would be large compared with the length of the column, and the linear assumption would not be anymore valid.

Figure 12 gives plots of  $P$  vs  $w_m$  at each fixed time  $t$ . The relationship between them is determined from Eq. (25g). Also, the

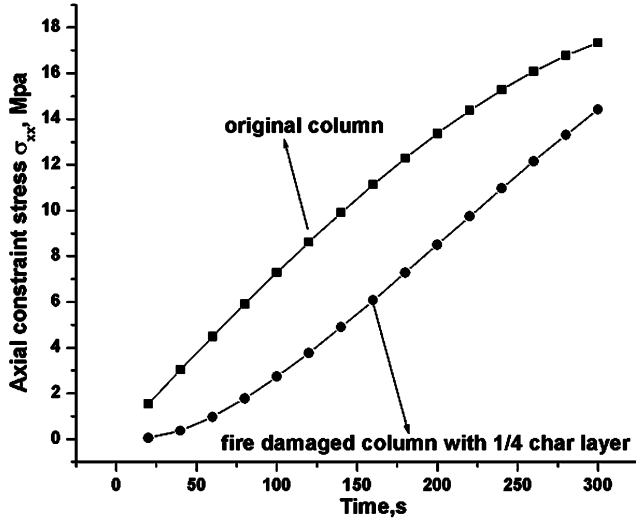


Fig. 13 Axial constraint stress  $\sigma_{xx}^{\text{con}}$  vs time for the charred and the original columns subjected to heat flux  $Q = 5 \text{ kW/m}^2$  (constrained, immovable ends case).

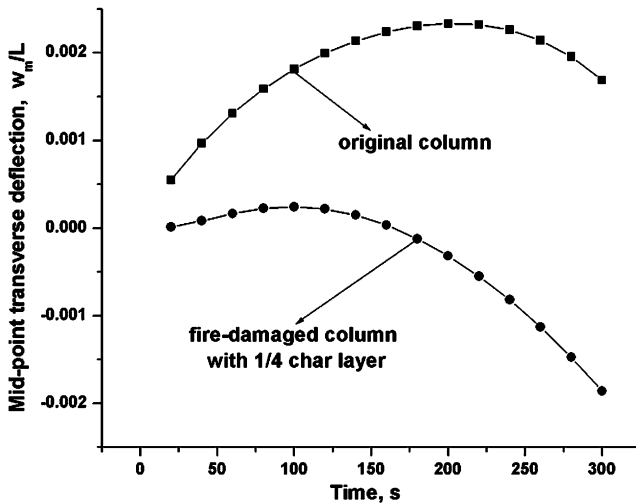


Fig. 14 Midpoint transverse deflection vs time for the charred and the original columns subjected to heat flux  $Q = 5 \text{ kW/m}^2$  (constrained, immovable ends case).

end of the column can move freely, hence the constraint boundary conditions are released, and the initial  $w_m$  was calculated from the linear analysis. In Fig. 12, the applied axial force is normalized by the Euler critical load at room temperature  $P_E$  and  $w_m$  is normalized by the length of the column. The figure shows that at the beginning of heat exposure (e.g.,  $t = 20 \text{ s}$  curve), the temperature of the column is relatively low and the axial force  $P$  increases initially with only a small bending deflection; as  $P$  approaches  $P_E$ , the transverse deflection increases rapidly, with  $P$  becoming asymptotic to  $P_E$ . The response is very similar with the typical Euler buckling response, which means that the bending moment influence is very trivial at the beginning of heat exposure; With heat  $t$  increasing further, the load-deflection curve “bends over” much earlier in the response, and the beam behaves much like an “imperfect” column. Eventually, in all cases, the axial force approaches  $P_E$  as the midspan transverse deflection becomes large. The temperature variation through the thickness has effectively an analogous role for the column as that of an imperfection on a mechanically loaded column. That is, both a temperature change through the thickness and an initial imperfection would cause a moment that bends the column from the instant any load, whether thermal or mechanical, is applied.

The temperature in the undamaged layer of the charred column is lower than the original column without the fire-damaged layer based

on Figs. 5 and 6. It is necessary to compare the axial stresses and the midpoint deflections for the charred and the original columns. In Fig. 13, the constraint axial stress  $\sigma_{xx}^{\text{con}}$  vs time for both the original and the charred columns, is shown. The two columns are constrained at both ends and exposed to a heat flux  $Q = 5 \text{ kW/m}^2$ . For the charred column with  $\frac{1}{4}$  thickness fire-damaged layer, the axial constraint stress is lower than in the original column, although the mechanical properties of fire-damaged material are neglected in the analysis. In Fig. 14, the midpoint transverse deflections for both columns under constraint forces are shown. The midpoint deflections are normalized with the length of the columns. From Fig. 14, we see that the midpoint transverse deflection of the fire-damaged column is always smaller than that of the original one. The reason for such a difference is due to the temperature distributions. For the original column, it should be noted that the midpoint transverse deflection is always positive, the thermal moment dominates because the temperature is much higher without the fire-damaged layer protection compared with the charred column. For the fire-damaged column, the temperature is lower and  $M_z^e$  has more influence on the transverse deflection  $w$  compared with the original column. This is because a fire-damaged (char) layer exists and the stiffness for this layer is so small that it is neglected, but when the eccentric distance is determined, the thickness of this layer should be accounted and therefore makes the eccentric moment  $M_z^e$  dominate the transverse deflection  $w$ .

#### IV. Conclusions

The thermal buckling/bending problem of a composite column with a char layer due to exposure to fire is studied. Two cases are considered: when the column is axially restrained (immovable ends) or when there is no restraint and an axial applied force is applied. First, the temperature distribution is obtained by solving the bimaterial heat conduction problem in closed form. Subsequently, this temperature profile is used in conjunction with the temperature-dependent moduli of the composite undamaged layer to obtain the buckling response; in this phase the mechanical properties of the char layer are neglected. In addition, the thermal buckling analysis includes the effect of transverse shear. To see the influence of the char layer on the temperature distribution and the thermal buckling response, the same problem is also solved for the original column (without a char layer). From the results obtained, we can draw the following specific conclusions:

1) The temperature in the undamaged layer of the “charred” column is much lower than that in the original column due to the thermal protection of the char layer; and the net temperature variation in the undamaged layer is lower than the corresponding net temperature variation in the original column.

2) For the columns under heat exposure, there exist two possible transverse deformation modes, one is the column bending toward the heat source, the other is the column bending away from the heat source. The transverse deformation is determined by the overall moment, and which direction the column bends is determined by the competition between  $M_z^T$  and  $M_z^e$ .

3) For the constrained column (immovable ends), the results show that the column bends toward to the heat source at the beginning of heat exposure due to the dominance of  $M_z^T$ ; with increasing heat exposure time, the column bends away from the heat source, as the eccentricity moment begins to dominate.

4) For the column under heat exposure which is free to move axially (unconstrained case), the response is similar to that of an imperfect column. The temperature distribution through the thickness has effectively a role analogous to that of an imperfection on a mechanically loaded column.

5) If both columns are restrained at both ends (constrained, immovable ends case), the axial restraint stress of the charred column is less than that of the original column and the midpoint transverse deflection of the charred column under the constraint force is smaller than that of the original column.

### Acknowledgments

The financial support of the Office of Naval Research, Grant N00014-03-1-0189, and the interest and encouragement of the Grant Monitors, Patrick C. Potter and Luise Couchman is gratefully acknowledged.

### References

- [1] Sorathia, U., Rollhauser, C. M., and Hughes, W. A., "Improved Fire Safety of Composites for Naval Applications," *Fire and Materials*, Vol. 16, No. 3, 1992, pp. 119–125.
- [2] Sorathia, U., Lyon, R., Gann, R., and Gritz, L., "Materials and Fire Threat," *SAMPE Journal*, Vol. 32, No. 3, 1996, pp. 8–15.
- [3] Egglestone, G. T., and Turley, D. M., "Flammability of GRP for Use in Ship Superstructures," *Fire and Materials*, Vol. 18, No. 4, 1994, pp. 255–260.
- [4] Scudamore, M. J., "Fire Performance Studies on Glass-Reinforced Plastic Laminates," *Fire and Materials*, Vol. 18, No. 5, 1994, pp. 313–325.
- [5] Gibson, A. G., and Hume, J., "Fire Performance of Composite Panels for Large Marine Structures," *Plastics, Rubber and Composites Processing and Applications*, Vol. 23, No. 3, 1995, pp. 175–183.
- [6] Brown, J. R., and Mathys, Z., "Reinforcement and Matrix Effects on the Combustion Properties of Glass Reinforced Polymer Composites," *Composites, Part A: Applied Science and Manufacturing*, Vol. 28, No. 7, 1997, pp. 675–681.
- [7] Mouritz, A. P., and Gardiner, C. P., "Compression Properties of Fire-Damaged Polymer Sandwich Composites," *Composites, Part A: Applied Science and Manufacturing* Vol. 33, No. 5, 2002, pp. 609–620.
- [8] Kulkarni, A. P., and Gibson, R. F., "Nondestructive Characterization of Effects of Temperature and Moisture on Elastic Moduli of Vinyl Ester Resin and E-Glass/Vinylester Composite," *Proceedings of the American Society of Composites 18th Annual Technical Conference*, University of Florida, Gainesville, FL, 2003.
- [9] Simitzes, G. J., *An Introduction to the Elastic Stability of Structures*, Krieger, Malabar, FL, 1986.
- [10] Huang, H., and Kardomateas, G. A., "Buckling and Initial Postbuckling Behavior of Sandwich Beams Including Transverse Shear," *AIAA Journal*, Vol. 40, No. 11, 2002, pp. 2331–2335.

K. Shivakumar  
Associate Editor